

Energy Dependence of Pion and Kaon Production in Central Pb+Pb Collisions

The NA49 Collaboration

Abstract

Results on the energy dependence of charged pion and kaon production in central Pb+Pb collisions at 40, 80 and 158 $A\cdot\text{GeV}$ are presented and compared with data at lower and higher energies. The mean pion multiplicity increases approximately linearly with $s^{1/4}$ with a change of slope around 40 $A\cdot\text{GeV}$. The change from pion suppression with respect to p+p interactions, as observed at low collision energies, to pion enhancement at high energies also occurs at about 40 $A\cdot\text{GeV}$. A non-monotonic energy dependence of the ratio of K^+ to π^+ yields is observed, with a maximum close to 40 $A\cdot\text{GeV}$, followed by a nearly constant value at higher energies. The measured dependences are consistent with the hypothesis, derived within a Statistical Model of the Early Stage of nucleus-nucleus reactions, that a transient state of deconfined matter is created in Pb+Pb collisions for energies larger than about 40 $A\cdot\text{GeV}$.

The NA49 Collaboration

S.V. Afanasiev⁹, T. Anticic²⁰, D. Barna⁵, J. Bartke⁷, R.A. Barton³, M. Behler¹⁵, L. Betev¹⁰, H. Bialkowska¹⁷, A. Billmeier¹⁰, C. Blume⁸, C.O. Blyth³, B. Boimska¹⁷, M. Botje¹, J. Bracinik⁴, R. Bramm¹⁰, R. Brun¹¹, P. Bunčić^{10,11}, V. Cerny⁴, J.G. Cramer¹⁹, P. Csató⁵, P. Dinkelaker¹⁰, V. Eckardt¹⁶, P. Filip¹⁶, H.G. Fischer¹¹, Z. Fodor⁵, P. Foka⁸, P. Freund¹⁶, V. Friese¹⁵, J. Gál⁵, M. Gaździcki¹⁰, G. Georgopoulos², E. Gładysz⁷, S. Hegyi⁵, C. Höhne¹⁵, G. Igo¹⁴, P.G. Jones³, K. Kadija^{11,20}, A. Karev¹⁶, V.I. Kolesnikov⁹, T. Kollegger¹⁰, M. Kowalski⁷, I. Kraus⁸, M. Kreps⁴, M. van Leeuwen¹, P. Lévai⁵, A.I. Malakhov⁹, S. Margetis¹³, C. Markert⁸, B.W. Mayes¹², G.L. Melkumov⁹, A. Mischke⁸, J. Molnár⁵, J.M. Nelson³, G. Pála⁵, A.D. Panagiotou², K. Perl¹⁸, A. Petridis², M. Pikna⁴, L. Pinsky¹², F. Pühlhofer¹⁵, J.G. Reid¹⁹, R. Renfordt¹⁰, W. Retyk¹⁸, C. Roland⁶, G. Roland⁶, A. Rybicki⁷, T. Sammer¹⁶, A. Sandoval⁸, H. Sann⁸, N. Schmitz¹⁶, P. Seyboth¹⁶, F. Siklér⁵, B. Sitar⁴, E. Skrzypczak¹⁸, G.T.A. Squier³, R. Stock¹⁰, H. Ströbele¹⁰, T. Susa²⁰, I. Szentpétery⁵, J. Sziklai⁵, T.A. Trainor¹⁹, D. Varga⁵, M. Vassiliou², G.I. Veres⁵, G. Vesztergombi⁵, D. Vranić⁸, S. Wenig¹¹, A. Wetzler¹⁰, C. Whitten¹⁴, I.K. Yoo¹⁵, J. Zaranek¹⁰, J. Zimányi⁵

¹NIKHEF, Amsterdam, Netherlands.

²Department of Physics, University of Athens, Athens, Greece.

³Birmingham University, Birmingham, England.

⁴Comenius University, Bratislava, Slovakia.

⁵KFKI Research Institute for Particle and Nuclear Physics, Budapest, Hungary.

⁶MIT, Cambridge, USA.

⁷Institute of Nuclear Physics, Cracow, Poland.

⁸Gesellschaft für Schwerionenforschung (GSI), Darmstadt, Germany.

⁹Joint Institute for Nuclear Research, Dubna, Russia.

¹⁰Fachbereich Physik der Universität, Frankfurt, Germany.

¹¹CERN, Geneva, Switzerland.

¹²University of Houston, Houston, TX, USA.

¹³Kent State University, Kent, OH, USA.

¹⁴University of California at Los Angeles, Los Angeles, USA.

¹⁵Fachbereich Physik der Universität, Marburg, Germany.

¹⁶Max-Planck-Institut für Physik, Munich, Germany.

¹⁷Institute for Nuclear Studies, Warsaw, Poland.

¹⁸Institute for Experimental Physics, University of Warsaw, Warsaw, Poland.

¹⁹Nuclear Physics Laboratory, University of Washington, Seattle, WA, USA.

²⁰Rudjer Boskovic Institute, Zagreb, Croatia.

I. INTRODUCTION

The primary purpose of the heavy ion programme at the CERN SPS is the search for a transient deconfined state of strongly interacting matter during the early stage of nucleus–nucleus collisions [1]. When a sufficiently high initial energy density is reached, the formation of such a state of quasi free quarks and gluons, the quark gluon plasma (QGP), is expected. A key problem is the identification of experimental signatures of QGP creation [2]. Numerous proposals were discussed in the past [3], but the significance of these signals has come under renewed scrutiny. A possible, promising strategy is a study of the energy dependence of pion and strangeness yields. It was suggested [4,5] that the transition may lead to anomalies in this dependence: a steepening of the increase of the pion yield and a non monotonic behaviour of the strangeness to pion ratio. The space–time evolution of the created fireball [6] and the event–by–event fluctuations [7] may also be sensitive to crossing the transition region.

First experimental results from Pb+Pb (Au+Au) collisions at top SPS (158 $A\cdot\text{GeV}$) and AGS (11 $A\cdot\text{GeV}$) energies have suggested [4] that anomalies in pion and strangeness production may be located between these energies. The study of this hypothesis is the motivation for a dedicated energy scan at the CERN SPS [8]. Within this ongoing project NA49 has recorded central Pb+Pb collisions at 40 and 80 $A\cdot\text{GeV}$ during the heavy ion runs in 1999 and 2000, respectively. The data at the top SPS energy (158 $A\cdot\text{GeV}$) were taken in previous SPS runs. In this paper we report final results on the energy dependence of charged pion and kaon production. A preliminary analysis was presented in Refs. [9,10]. Pseudorapidity spectra of charged particles produced in Pb+Pb collisions at 40 and 158 $A\cdot\text{GeV}$ were recently published by the NA50 experiment [11].

The energy scan programme at the CERN SPS will be completed in 2002 by taking data at 20 and 30 $A\cdot\text{GeV}$.

II. EXPERIMENTAL SET–UP

The NA49 experimental set–up [12] is shown in Fig. 1. It consists of four large volume Time Projection Chambers (TPCs). Two of these, the Vertex TPCs (VTPC-1 and VTPC-

2), are placed in the magnetic field of two super-conducting dipole magnets. This allows separation of positively and negatively charged tracks and a precise measurement of the particle momenta p with a resolution of $\sigma(p)/p^2 \cong (0.3-7) \cdot 10^{-4} (\text{GeV}/c)^{-1}$. The other two TPCs (MTPC-L and MTPC-R), positioned downstream of the magnets were optimised for high precision measurement of the ionization energy loss dE/dx (relative resolution of about 4%) which provides a means of determining the particle mass. The acceptance of these TPCs starts at midrapidity for kaons. The particle identification capability of the MTPCs is augmented by two Time of Flight (TOF) detector arrays with a resolution $\sigma_{tof} \cong 60$ ps. The combined TPC and TOF information allows for the measurement of charged kaon spectra at midrapidity. In order to optimise the NA49 acceptance at 40 and 80 $A \cdot \text{GeV}$ the magnetic fields in the VTX-1 and VTX-2 magnets were lowered in proportion to the beam energy. The setting at 158 $A \cdot \text{GeV}$ was: $B(\text{VTX-1}) \cong 1.5$ T and $B(\text{VTX-2}) \cong 1.1$ T. Data were taken for both field polarities.

The target, a thin lead foil ($224 \text{ mg}/\text{cm}^2$, $\cong 1\%$ of the interaction length), was positioned about 80 cm upstream from VTPC-1.

Central collisions were selected by a trigger using information from a downstream calorimeter (VCAL), which measured the energy of the projectile spectator nucleons. The geometrical acceptance of the VCAL calorimeter was adjusted for each energy in order to cover the projectile spectator region by a proper setting of a collimator (COLL) [12,13].

III. ANALYSIS

Raw K^+ and K^- yields were extracted from fits of the distributions of dE/dx and tof (where available) in narrow bins of momentum and transverse momentum p_T . The resolution of the dE/dx measurement alone allows for hadron identification in the region $p > 4 \text{ GeV}/c$, i.e. above midrapidity for kaons. The spectra at midrapidity are obtained using combined dE/dx and tof information ($tof + dE/dx$ analysis). The resulting distributions were then corrected for geometrical acceptance, losses due to in-flight decays and reconstruction efficiency. The first two corrections are calculated using the detector simulation package GEANT [15]. The procedure used for the efficiency calculation is

discussed below, in the context of the pion analysis.

For pions the acceptance of the dE/dx method is limited to the high p_T region around midrapidity and therefore a somewhat different procedure was used to obtain their spectra. Yields of all negatively charged particles were determined as a function of rapidity (calculated assuming the π -mass) and p_T and corrected for the geometrical acceptance. The contamination of K^- , \bar{p} and e^- from the interaction vertex as well as non-vertex hadrons originating from strange particle decays and secondary interactions was subtracted. (The π^+ spectra were not analysed, because the positive particles have a significant contribution of protons.) Two different methods were used here. In the first one each track measured in the TPCs was extrapolated back to the target plane. The distance between the track and the interaction vertex was calculated in this plane (track impact parameter). The impact parameter distributions were used to establish cuts for selection of tracks from the interaction vertex and to estimate the contribution of remaining non-vertex tracks. A correction for K^- contamination was calculated using parametrised K^- spectra. In the second method all tracks fitted to the interaction vertex were accepted. The necessary corrections were calculated based on a VENUS [14] simulation of central Pb+Pb collisions. The VENUS events were processed by GEANT [15] and the NA49 software which simulates the TPC response and produces files in the raw data format. These events were reconstructed and the reconstructed tracks were matched to the VENUS input. The obtained correction was scaled by a factor which matches the simulated VENUS and the measured hadron yields. The corrections determined using both methods are compatible and amount to 20–25%. The VENUS based correction is used for the data presented in this paper.

The final spectra were also corrected for inefficiencies in the tracking and losses due to quality cuts. These losses were determined using the ‘embedding’ method. Events containing a few tracks were generated and processed by the simulation software. The resulting raw data were embedded into real events. The combined raw data were reconstructed and the input tracks were matched with the reconstructed ones. The calculated inefficiencies are about 5%.

In order to reduce the systematic errors, the analysis has been restricted to regions of

phase space where the background and efficiency corrections are small and approximately uniform. The systematic errors were estimated to be below 10%. This estimate is based on the comparison of results obtained using different detectors (TOF, TPC), and varying cuts and correction strategies (see above). Additionally, data taken at the two magnetic field polarities were analysed and the results were found to agree within 5%. Note that the same experimental procedure was used to obtain results at all three energies. Thus to a large extent the systematic uncertainties are common for the NA49 measurements.

The average number of wounded nucleons [16] $\langle N_W \rangle$ (the notation $\langle \dots \rangle$ will be used to denote the mean multiplicity in full phase space throughout the paper) as given in Table I was not directly measured but it was calculated using the Fritiof model [17]. From all generated events a fraction with the smallest number of projectile spectators was selected. The cut on the number of projectile spectators was adjusted such that the selected fraction was equal to the fraction of all inelastic interactions accepted by the central trigger. The value of $\langle N_W \rangle$ was then calculated for the Fritiof Pb+Pb collisions selected in this way. Finally it was checked that the $\langle N_W \rangle$ value for central Pb+Pb collisions at 158 A·GeV agrees (within several per cent) with the number of net baryons determined [18] in the participant domain (in the rapidity interval $-2.6 < y < 2.6$) for these collisions.

Note that in this paper y denotes the rapidity of a particle in the collision c.m. system.

Table I summarises the parameters characterising the data samples used in this analysis.

IV. RESULTS

Spectra of transverse mass $m_T = \sqrt{p_T^2 + m^2}$ (m is the rest mass of the particle) for K^+ , K^- (*tof + dE/dx* analysis) and π^- mesons produced near midrapidity ($|y| < 0.1$ for kaons and $0 < y < 0.2$ for pions) in central Pb+Pb collisions at 40, 80 and 158 A·GeV are shown in Fig. 2. The solid lines indicate a fit of the function

$$\frac{dn}{m_T dm_T dy} = C \cdot \exp(-m_T/T) \quad (1)$$

to the data in the range $0.2 \text{ GeV} < m_T - m < 0.7 \text{ GeV}$. The values obtained for the inverse slope parameter T are presented in Table II. The T parameter is smaller for pions

than for kaons. A weak increase of T with increasing energy is suggested by the pion data, whereas no significant change is seen for kaons.

The rapidity distributions dn/dy plotted in Fig. 3 were obtained by summing of the measured m_T spectra and using the fitted exponential function (Eq. 1) to extrapolate to full m_T . For most bins the necessary correction is small ($\cong 5\%$). The values of dn/dy at midrapidity ($|y| < 0.6$) are given in Table II. An increase of rapidity density with energy is seen for all particles. The rapidity spectra were parameterised by the sum of two-Gauss distributions placed symmetrically with respect to midrapidity:

$$\frac{dn}{dy} = N \cdot \left[\exp\left(\frac{(y - y_0)^2}{2\sigma^2}\right) + \exp\left(\frac{(y + y_0)^2}{2\sigma^2}\right) \right]. \quad (2)$$

The results of the fits are indicated by solid lines in Fig. 3 and the obtained values of the parameters N, y_0 and σ are given in Table III. Since both y_0 and σ increase with increasing energy, the width of the observed rapidity distributions clearly increases with energy. The mean multiplicities in full phase space were calculated by integrating the parametrised rapidity spectra. The resulting numbers are given in Table II. The mean multiplicity of π^+ mesons given in Table II was calculated by scaling $\langle\pi^-\rangle$ by the π^+/π^- ratio (0.91, 0.94 and 0.97 at 40, 80 and 158 A-GeV, respectively) measured in the region where both dE/dx and tof measurements are available. Results on dn/dy and inverse slope parameters near midrapidity at 158 A-GeV are in agreement (within relatively large errors) with the previously published measurements [19].

V. ENERGY DEPENDENCE

The energy dependence of the mean pion multiplicity $\langle\pi\rangle = 1.5 \cdot (\langle\pi^+\rangle + \langle\pi^-\rangle)$ is shown in Fig. 4. In this figure the ratio $\langle\pi\rangle/\langle N_W\rangle$ is plotted as a function of the collision energy, expressed by Fermi's measure [20]: $F \equiv (\sqrt{s} - 2m_N)^{3/4}/\sqrt{s}^{1/4}$, where \sqrt{s} is the c.m.s. energy per nucleon-nucleon pair and m_N the rest mass of the nucleon. Measurements by NA49 are compared to results from other experiments on central nucleus-nucleus collisions [4,21,22] and to a compilation of data from p+p(\bar{p}) interactions (see references in [4]).

One observes that the mean pion multiplicity in p+p(\bar{p}) interactions is approximately proportional to F ; the dashed line in Fig. 4 indicates a fit of the form $\langle\pi\rangle/\langle N_W\rangle = a \cdot F$

to the data, yielding $a = 1.025 \pm 0.005 \text{ GeV}^{-1/2}$. In the case of central A+A collisions the dependence is more complicated. Below 40 A·GeV the ratio $\langle\pi\rangle/\langle N_W\rangle$ in A+A collisions is lower than in p+p interactions (pion suppression), although the slopes of the dependence on F are similar. An increase of the slope is observed at about 40 A·GeV and at higher energies the $\langle\pi\rangle/\langle N_W\rangle$ ratio is higher in A+A collisions than in p+p(\bar{p}) interactions (pion enhancement). Starting from the top CERN SPS energy up to RHIC energies [22] the $\langle\pi\rangle/\langle N_W\rangle$ ratio increases again in proportion to F . The fit to the 158 A·GeV data point and RHIC results (solid line in Fig. 4) yields a slope parameter $a = 1.34 \pm 0.06 \text{ GeV}^{-1/2}$. The transition from pion suppression to pion enhancement is demonstrated more clearly in the insert of Fig. 4, where the difference between the $\langle\pi\rangle/\langle N_W\rangle$ ratio for A+A and p+p interactions (parametrised by the straight line fit) is plotted as a function of F up to the top CERN SPS energy.

Midrapidity and full phase space kaon to pion ratios are shown as a function of \sqrt{s} in Figs. 5 and 6 [4,21,23], respectively. A monotonic increase with \sqrt{s} of K^-/π^- is measured. For the K^+/π^+ ratio, a very different behaviour is observed: a steep increase in the low (AGS [21]) energy region is followed by a rapid turnover (around 40 A·GeV) into a decreasing trend. For comparison the results on the $\langle K^+\rangle/\langle\pi^+\rangle$ ratio in p+p interactions [4] are also shown in Fig. 6. The p+p data have rather large error bars [4], but suggest a monotonic increase of the ratio. It should be noted that the energy dependence of the $\langle K^+\rangle/\langle\pi^+\rangle$ ratio is expected to be approximately (within of about 10%) independent of the charge composition of colliding nuclei [24].

The energy dependence of the K^-/K^+ ratio at midrapidity is shown in Fig. 7. The ratio increases with \sqrt{s} from about 0.15 at low AGS energy [21] to about 0.5 at SPS energies and reaches about 0.9 at RHIC [23].

The difference between the dependence of K^+ and K^- yields on \sqrt{s} can be attributed to their different sensitivity to the baryon density. Kaons (K^+ and K^0) carry a dominant fraction of all produced \bar{s} -quarks (more than 95% in Pb+Pb collisions at 158 A·GeV if open strangeness is considered). Therefore the K^+ yield ($\langle K^+\rangle \cong \langle K^0\rangle$ in approximately isospin symmetric collisions of heavy nuclei) is nearly proportional to the total strangeness production and only weakly sensitive to the baryon density. As a significant fraction of s -

quarks (e.g. about 50% in central Pb+Pb collisions at 158 $A\cdot\text{GeV}$) is carried by hyperons, the number of produced antikaons (K^- and \bar{K}^0) is sensitive to both the strangeness yield and the baryon density.

In Fig. 8 an alternative measure of the strangeness to pion ratio, $E_S = (\langle\Lambda\rangle + \langle K + \bar{K}\rangle)/\langle\pi\rangle$, is plotted as a function of F for A+A collisions [21] and p+p interactions [4]. For A+A collisions the Λ multiplicity, when not published, (e.g. for the NA49 points) was estimated as $\langle\Lambda\rangle = (\langle K^+\rangle - \langle K^-\rangle)/0.8$, based on strangeness conservation and approximate isospin symmetry of the colliding nuclei [24]. The wealth of data on Λ and K_S^0 production in p+p interactions [4] allows a much more precise determination of E_S (open circles in Fig. 8) than of the $\langle K^+\rangle/\langle\pi^+\rangle$ ratio (open circles in Fig. 6). By construction, E_S should be almost independent (an expected variation of several per cent) of the charge composition of colliding nuclei. One may conclude from Figs. 6 and 8 that a non-monotonic energy dependence (or a sharp turnover) of the total strangeness to pion ratio appears to be a special property of heavy ion collisions, which is not observed in elementary interactions.

VI. COMPARISON WITH MODELS

The energy dependence of pion and strangeness yields was discussed within various approaches to nucleus–nucleus collisions. In this section we summarise the published results.

The Statistical Model of the Early Stage (SMES) [5] is based on the assumption that the system created at the early stage (be it confined matter or a QGP) is in equilibrium and a transition from a reaction with purely confined matter to a reaction with a QGP at the early stage occurs where the transition temperature T_C is reached. For T_C values of 170–200 MeV the transition region ranges between 15–60 $A\cdot\text{GeV}$ [5].

Due to the assumed generalised Fermi–Landau initial conditions [25,5] the $\langle\pi\rangle/\langle N_W\rangle$ ratio in the model increases approximately linearly with F outside the transition region. The slope parameter is proportional to $g^{1/4}$ [26], where g is an effective number of internal degrees of freedom at the early stage. In the transition region a steepening of the

pion energy dependence is expected, because of activation of a large number of partonic degrees of freedom. This is, in fact, observed in the data on central Pb+Pb (Au+Au) collisions, where the steepening takes place in the range of low CERN SPS energies, close to 40 A·GeV (see Fig. 4). The linear dependence on F is obeyed by the data at lower and higher (including RHIC) energies. An increase of the slope by a factor of about 1.25 is measured (see Sect. V), which corresponds to an increase of the effective number of internal degrees of freedom by a factor of $1.25^4 \cong 2.5$, within the SMES. The final results presented here confirm an early estimate [26] which was made when much less data was available.

The $\langle K^+ \rangle / \langle \pi^+ \rangle$ and E_S ratios are roughly proportional to the total strangeness to entropy ratio which, in the SMES model, is assumed to be preserved from the early stage till freeze-out. At low collision energies the strangeness to entropy ratio steeply increases with collision energy, due to the low temperature at the early stage ($T < T_C$) and the high mass of the carriers of strangeness ($m_S \cong 500$ MeV, the kaon mass) in the confined state. When the transition to a QGP is crossed ($T > T_C$), the mass of the strangeness carriers is significantly reduced ($m_S \cong 170$ MeV, the strange quark mass). Due to the low mass ($m_S < T$) the strangeness yield becomes (approximately) proportional to the entropy, and the strangeness to entropy (or pion) ratio is independent of energy. This leads to a "jump" in the energy dependence from the larger value for confined matter at T_C to the QGP value. Thus, within the SMES, the measured non-monotonic energy dependence of the strangeness to entropy ratio followed by a saturation at the QGP value (see Figs. 6 and 8) is a direct consequence of the onset of deconfinement taking place at about 40 A·GeV.

Numerous models have been developed to explain reactions of heavy nuclei without explicitly invoking a transient QGP phase. The simplest one is the statistical hadron gas model [27] where independent of the collision energy the hadrochemical freeze-out creates a hadron gas in equilibrium [28]. The temperature, baryon chemical potential and hadronization volume are free parameters of the model, which are fitted to the data at each energy. In this formulation, the hadron gas model does not predict the energy dependence of hadron production. Recently, an extension of the model was proposed, in

which it is assumed that the values of the thermal parameters (temperature and baryon chemical potential) evolve smoothly with the collision energy [29]. The energy dependence calculated within this extended hadron gas model for the $\langle K^+ \rangle / \langle \pi^+ \rangle$ ratio is compared to the experimental results in Fig. 9. Due to its construction, the prevailing trend in the data is reproduced by the model, but the decrease of the ratio between 40 and 158 $A \cdot \text{GeV}$ is not well described. The measured strangeness to pion yield in central Pb+Pb collisions at 158 $A \cdot \text{GeV}$ is about 25% lower than the expectation for the fully equilibrated hadron gas [29,30].

Several dynamical hadron–string models have been developed to study hadron production in A+A collisions. These models treat the elementary collisions within a string–hadronic framework as a starting point. The models are then extended with effects which are expected to be relevant in A+A collisions (such as string–string interactions and hadronic rescattering). The predictions of RQMD [31,32] and UrQMD [33,34] models are shown in Fig. 9. It is seen that RQMD, like the hadron gas model, fails to describe the decrease of the $\langle K^+ \rangle / \langle \pi^+ \rangle$ ratio in the SPS energy range. The UrQMD model predicts a ratio which, above $\sqrt{s} \cong 5 \text{ GeV}$, does not show any sizable energy dependence and which is significantly lower (e.g. by about 40% at 40 $A \cdot \text{GeV}$) than the data. This is mainly due to the fact that UrQMD overestimates pion production at SPS energies by more than 30% [34].

The RQMD prediction of the energy dependence of the K^+/π^+ ratio at midrapidity is shown in Fig 10. The model also fails to reproduce these results. In addition, Fig. 10 presents the prediction of the HSD model [35] (another version of the dynamical hadron–string approach) which shows a monotonic increase of the K^+/π^+ ratio with energy. This trend is very different from the measured one.

VII. SUMMARY

Results on charged pion and kaon production in central Pb+Pb collisions at 40, 80 and 158 $A \cdot \text{GeV}$ were presented. The change from pion suppression at low collision energies to pion enhancement at high energies is located to occur at about 40 $A \cdot \text{GeV}$. A non–

monotonic energy dependence of the $\langle K^+ \rangle / \langle \pi^+ \rangle$ ratio is observed. A maximum is found close to 40 $A \cdot \text{GeV}$ followed by a nearly constant value at higher energies. The observed behaviour can be understood within a Statistical Model of the Early Stage of nucleus–nucleus collisions if the assumption is made that a transient state of deconfined matter is created in Pb+Pb collisions for energies larger than about 40 $A \cdot \text{GeV}$. Models which do not include this assumption do not properly reproduce the measured energy dependence of pion and strangeness production.

Acknowledgements

This work was supported by the Director, Office of Energy Research, Division of Nuclear Physics of the Office of High Energy and Nuclear Physics of the US Department of Energy (DE-ACO3-76SFOOO98 and DE-FG02-91ER40609), the US National Science Foundation, the Bundesministerium für Bildung und Forschung, Germany, the Alexander von Humboldt Foundation, the UK Engineering and Physical Sciences Research Council, the Polish State Committee for Scientific Research (5 P03B 13820 and 2 P03B 02418), the Hungarian Scientific Research Foundation (T14920 and T23790), Hungarian National Science Foundation, OTKA, (F034707), the EC Marie Curie Foundation, and the Polish-German Foundation.

REFERENCES

- [1] for review see Proceedings of the 14th International Conference on Ultra-Relativistic Nucleus-Nucleus Collisions, Quark Matter 99, eds.: L. Riccati, M. Masera and E. Vercellin, Nucl. Phys. **A661** (1999).
- [2] J. C. Collins and M. J. Perry, Phys. Rev. Lett. **34**, 1353 (1975),
E. V. Shuryak, Phys. Rep. **61**, 71 (1980) and **115**, 151 (1984).
- [3] J. Rafelski and B. Müller, Phys. Rev. Lett. **48**, 1066 (1982),
T. Matsui and H. Satz, Phys. Lett. **B178** (1986) 416.
- [4] M. Gaździcki and D. Röhrich, Z. Phys. **C65**, 215 (1995); **C71**, 55 (1996) and refer-
ences therein.
- [5] M. Gaździcki and M. I. Gorenstein, Acta Phys. Polon. **B30**, 2705 (1999), and refer-
ences therein.
- [6] C.M. Hung and E. Shuryak, Phys. Rev. Lett. **75**, 4003 (1995).
- [7] M. Stephanov, K. Rajagopal and E. Shuryak, Phys. Rev. **D60**, 114028 (1999).
- [8] J. Bächler et al. (NA49 Collab.), *Searching for QCD Phase Transition*, Addendum-1
to Proposal SPSLC/P264, CERN/SPSC 97 (1997).
- [9] C. Blume et al. (NA49 Collab.), Nucl. Phys. **A698**, 104 (2002).
- [10] T. Kollegger et al. (NA49 Collab.), To appear in the proceedings of 6th International
Conference on Strange Quarks in Matter: 2001: A Flavorspace Odyssey (SQM2001),
Frankfurt, Germany, 25-29 Sep 2001, e-Print Archive: nucl-ex/0201019.
- [11] M. C. Abreu et al. (NA50 Collab.), Phys. Lett. **B530**, 33 (2002) and **B530**, 43 (2002).
- [12] S. Afanasiev et al. (NA49 Collab.), Nucl. Instrum. Meth. **A430**, 210 (1999).
- [13] H. Appelshauser et al. (NA49 Collab.), Eur. Phys. J. **A2**, 383 (1998).
- [14] K. Werner, Phys. Rep. **232**, 87 (1993).
- [15] GEANT-Detector Description and Simulation Tool, CERN Program Library Long

Writeup W5013.

- [16] A. Białas, M. Błeszyński and W. Czyż, Nucl. Phys. **B111** (1976) 461.
- [17] B. Andersson, G. Gustafson and Hong Pi, Z. Phys. **C57**, 485 (1993).
- [18] H. Appelshauser et al. (NA49 Collab.), Phys. Rev. Lett. **82**, 2471 (1999).
- [19] I. Bearden et al. (NA44 Collab.), Phys. Lett. **B471**, 6 (1999).
- [20] E. Fermi, Prog. Theor. Phys. **5**, 570 (1950).
- [21] L. Ahle et al. (E802 Collab.), Phys. Rev. **C57**, 466 (1998),
L. Ahle et al. (E802 Collab.), Phys. Rev. **C58**, 3523 (1998),
L. Ahle et al. (E802 Collab.), Phys. Rev. **C60**, 044904 (1999),
L. Ahle et al. (E866 Collab. and E917 Collab.), Phys. Lett. **B476**, 1 (2000),
L. Ahle et al. (E866 Collab. and E917 Collab.), Phys. Lett. **B490**, 53 (2000),
J. Barrette et al. (E877 Collab.), Phys. Rev. **C62**, 024901 (2000)
D. Pelte et al. (FOPI Collab.), Z. Phys. **A357**, 215 (1997).
- [22] B. B. Back et al. (PHOBOS Collab.), Phys. Rev. Lett. **85**, 3100 (2000) and Phys. Rev. Lett. **87**, 102303 (2001) and Phys. Rev. Lett. **88**, 022302 (2002),
The mean charged particle multiplicity in central Au+Au collisions at RHIC is published at $\sqrt{s_{NN}} = 130$ GeV, it is obtained by integrating the measured pseudorapidity distribution at $\sqrt{s_{NN}} = 200$ GeV and by extrapolating the midrapidity measurement at $\sqrt{s_{NN}} = 56$ GeV. From these results the contribution of charged kaons and protons is subtracted.
- [23] K. Adcox et al. (PHENIX Collab.), nucl-ex/0112006, to appear in Phys. Rev. Lett.,
B. B. Back et al. (PHOBOS Collab.), Phys. Rev. Lett. **87** (2001) 102301.
- [24] M. Gaździcki and O. Hansen, Nucl. Phys. **A528** (1991) 754.
- [25] E. Fermi, Prog. Theor. Phys. **5**, 570 (1950),
L. D. Landau, Izv. Akad. Nauk SSSR, Ser. Fiz. **17**, 51 (1953).
- [26] M. Gaździcki, Z. Phys. **C66**, 659 (1995).

- [27] R. Hagedorn, CERN report CERN-TH-7190-94 and Proceedings of NATO Advanced Study Workshop on Hot Hadronic Matter: Theory and Experiment, Divonne-les-Bains, Switzerland, 27 Jun - 1 Jul 1994, Hot Hadronic Matter, 13 (1994),
 J. Cleymans and H. Satz, Z. Phys. **C57** (1993) 135,
 J. Sollfrank, M. Gaździcki, U. Heinz and J. Rafelski, Z. Phys. **C61** (1994) 659,
 P. Braun–Munzinger, J. Stachel, J. Wessels and N. Xu, Phys. Lett. **B365** (1996) 1,
 G. D. Yen, M. I. Gorenstein, W. Greiner, S.N. Yang, Phys. Rev. **C56** (1997) 2210,
 G. D. Yen and M. I. Gorenstein, Phys. Rev. **C59** (1999) 2788.
- [28] R. Stock, Phys. Lett. **B456** (1999) 277.
- [29] J. Cleymans and K. Redlich, Phys. Rev. **C60**, 054908 (1999),
 P. Braun-Munzinger et al., Nucl. Phys. **A697**, 902 (2002).
- [30] F. Becattini, M. Gaździcki and J. Sollfrank, Eur. Phys. J. **C5**, 143 (1998).
- [31] H. Sorge, H. Stöcker and W. Greiner, Nucl. Phys. **A498**, 567c (1989),
 H. Sorge, Phys. Rev. **C52**, 3291 (1995).
- [32] F. Wang, H. Liu, H. Sorge, N. Xu and J. Yang, Phys. Rev. **C61**, 064904 (2000).
- [33] S. A. Bass et al. (UrQMD Collab.), Prog. Part. Nucl. Phys. **41**, 255 (1998).
- [34] H. Weber et al. (UrQMD Collab.), to be published.
- [35] W. Cassing, E.L. Bratkovskaya and S. Juchem, Nucl. Phys. **A674**, 249 (2000).

Table I

The number of analysed events, the cross section of selected central interactions as percentage of total inelastic cross section ($\sigma^{INEL} = 7.15$ b) and the mean number of wounded nucleons for the selected central Pb+Pb collisions at 40, 80 and 158 $A\cdot\text{GeV}$. The first error given in the last column is statistical, the second systematic.

Energy [$A\cdot\text{GeV}$]	Number of events	$\sigma^{CENT}/\sigma^{INEL}$ [%]	$\langle N_W \rangle$
40	$4 \cdot 10^5$	7.2	$349 \pm 1 \pm 5$
80	$3 \cdot 10^5$	7.2	$349 \pm 1 \pm 5$
158	$4 \cdot 10^5$	5.0	$362 \pm 1 \pm 5$

Table II

The inverse slope parameter T of the transverse mass spectra fitted in the interval $0.2 \text{ GeV} < m_T - m < 0.7 \text{ GeV}$ at midrapidity ($|y| < 0.1$ for kaons, $tof + dE/dx$ analysis, and $0 < y < 0.2$ for pions), the rapidity density dn/dy averaged over an interval $|y| < 0.6$ as well as total mean multiplicities of π^- , π^+ , K^- and K^+ mesons produced in central Pb+Pb collisions at 40, 80 and 158 A·GeV. The first error is statistical, the second systematic.

	40 A·GeV	80 A·GeV	158 A·GeV
$T(\pi^-)$ (MeV)	$169 \pm 2 \pm 10$	$179 \pm 3 \pm 10$	$180 \pm 3 \pm 10$
$T(K^+)$ (MeV)	$232 \pm 3 \pm 6$	$230 \pm 5 \pm 6$	$232 \pm 4 \pm 6$
$T(K^-)$ (MeV)	$226 \pm 3 \pm 6$	$217 \pm 3 \pm 6$	$226 \pm 9 \pm 6$
$dn/dy(\pi^-)$	$106.1 \pm 0.4 \pm 6$	$140.4 \pm 0.5 \pm 7$	$175.4 \pm 0.7 \pm 9$
$dn/dy(\pi^+)$	$96.6 \pm 0.4 \pm 6$	$132.0 \pm 0.5 \pm 7$	$170.1 \pm 0.7 \pm 9$
$dn/dy(K^+)$	$20.1 \pm 0.3 \pm 1.0$	$24.6 \pm 0.2 \pm 1.2$	$29.6 \pm 0.3 \pm 1.5$
$dn/dy(K^-)$	$7.58 \pm 0.12 \pm 0.4$	$11.7 \pm 0.10 \pm 0.6$	$16.8 \pm 0.2 \pm 0.8$
$\langle \pi^- \rangle$	$322 \pm 3 \pm 16$	$474 \pm 5 \pm 23$	$639 \pm 17 \pm 31$
$\langle \pi^+ \rangle$	$293 \pm 3 \pm 15$	$446 \pm 5 \pm 22$	$619 \pm 17 \pm 31$
$\langle K^+ \rangle$	$59.1 \pm 1.9 \pm 3$	$76.9 \pm 2 \pm 4$	$103.0 \pm 5 \pm 5$
$\langle K^- \rangle$	$19.2 \pm 0.5 \pm 1.0$	$32.4 \pm 0.6 \pm 1.6$	$51.9 \pm 1.9 \pm 3$

Table III

The fitted parameters of the two-Gauss parametrization (see text, Eq. 2) of rapidity distributions measured for π^- , K^- and K^+ mesons produced in central Pb+Pb collisions at 40, 80 and 158 $A\cdot\text{GeV}$. Only statistical errors are given.

	40 $A\cdot\text{GeV}$	80 $A\cdot\text{GeV}$	158 $A\cdot\text{GeV}$
$N(\pi^-)$	74.0 ± 0.5	97.0 ± 0.7	107.6 ± 1.8
$N(K^+)$	16.2 ± 0.4	19.3 ± 0.3	23.4 ± 0.6
$N(K^-)$	6.03 ± 0.13	9.16 ± 0.12	12.8 ± 0.3
$\sigma(\pi^-)$	0.872 ± 0.005	0.974 ± 0.007	1.18 ± 0.02
$\sigma(K^+)$	0.725 ± 0.016	0.792 ± 0.018	0.88 ± 0.04
$\sigma(K^-)$	0.635 ± 0.011	0.705 ± 0.010	0.81 ± 0.02
$y_0(\pi^-)$	0.666 ± 0.006	0.756 ± 0.006	0.72 ± 0.02
$y_0(K^+)$	0.694 ± 0.008	0.742 ± 0.008	0.839 ± 0.012
$y_0(K^-)$	0.569 ± 0.010	0.668 ± 0.005	0.727 ± 0.010

FIGURES

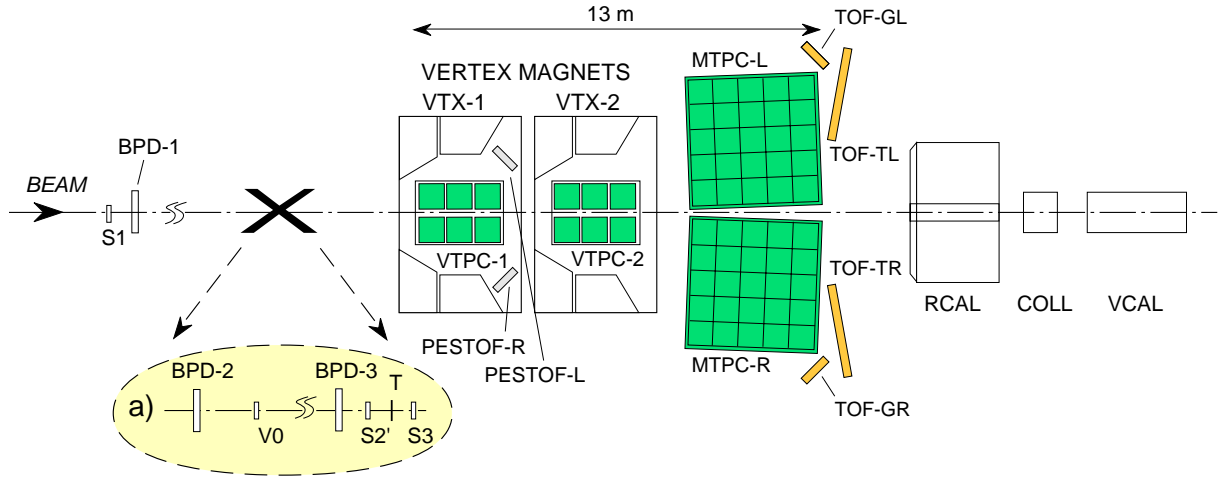


FIG. 1. The experimental set-up of the NA49 experiment [12].

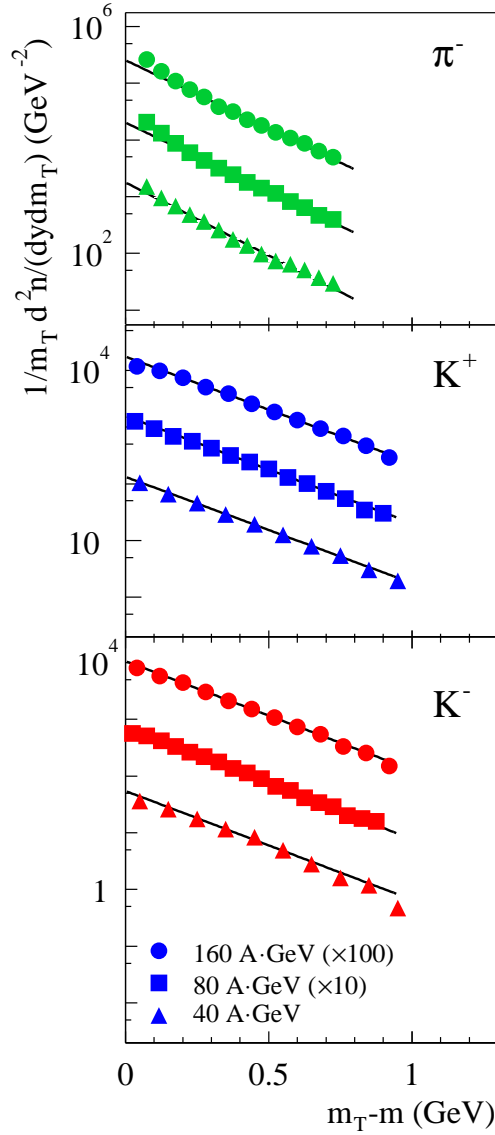


FIG. 2. The transverse mass spectra of π^- , K^+ and K^- mesons produced at midrapidity ($|y| < 0.1$ for kaons, $tof + dE/dx$ analysis, and $0 < y < 0.2$ for pions) in central Pb+Pb collisions at 40 (triangles), 80 (squares) and 158 (circles) $A \cdot \text{GeV}$. The values for 80 $A \cdot \text{GeV}$ and 158 $A \cdot \text{GeV}$ are scaled by factors of 10 and 100, respectively. The lines are exponential fits to the spectra (see text, Eq. 1) in the interval $0.2 \text{ GeV} < m_T - m < 0.7 \text{ GeV}$. Statistical errors are smaller than the symbol size. The systematic errors are $\pm 5\%$ in the region used for the fit and reach $\pm 10\%$ at the edges of the acceptance.

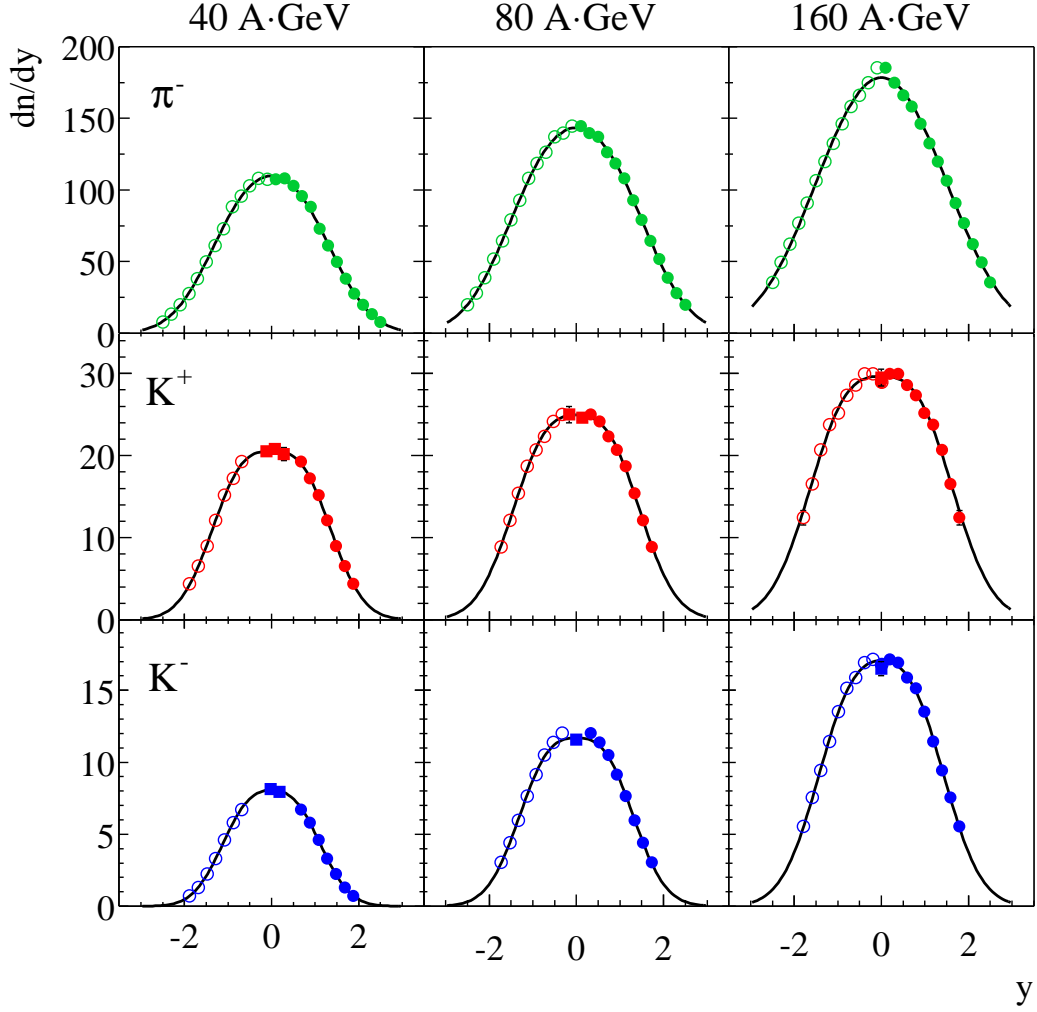


FIG. 3. The rapidity distributions of π^- , K^+ and K^- mesons produced in central Pb+Pb collisions at 40, 80 and 158 A-GeV. For kaons squares and circles indicate the results of $tof + dE/dx$ analysis and dE/dx analysis, respectively. The closed symbols indicate measured points, open points are reflected with respect to midrapidity. The lines indicate two-Gauss fits to the spectra (see Eq. 2). The plotted errors are statistical only, the systematic errors are $\pm 5\%$.

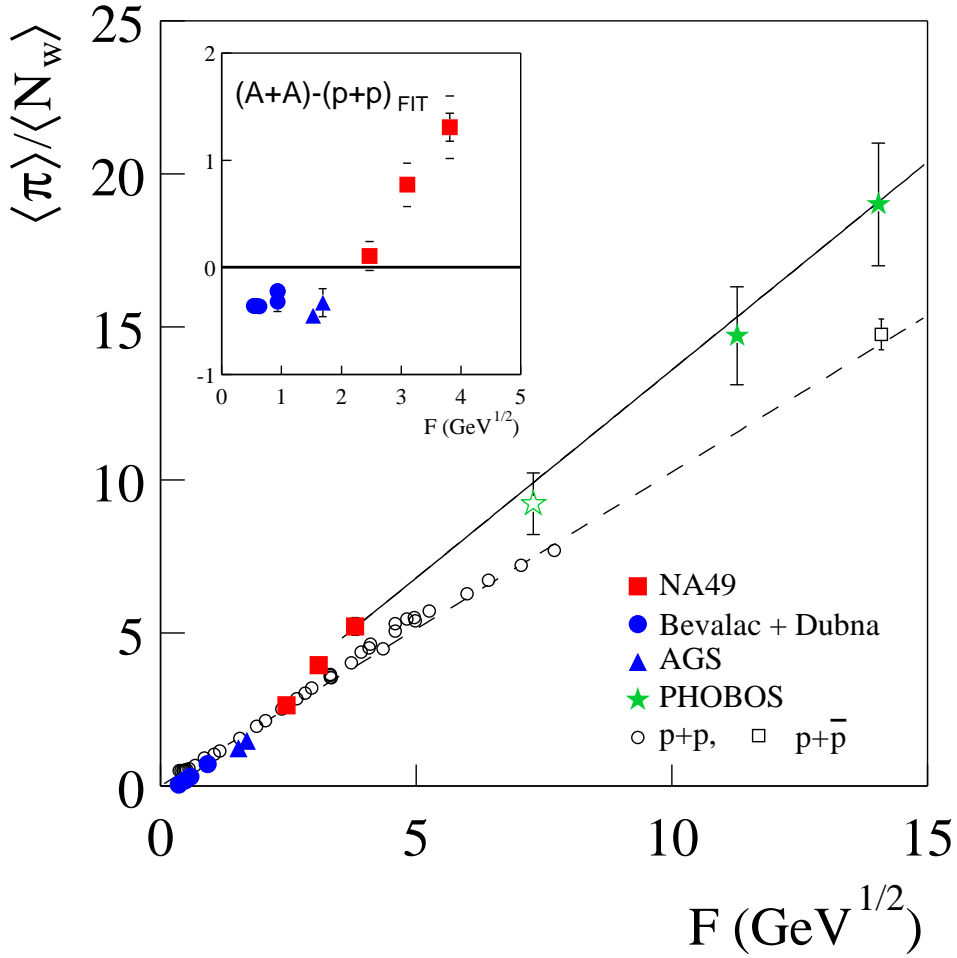


FIG. 4. The dependence of the total pion multiplicity per wounded nucleon on Fermi's energy measure F (see text for a definition) for central A+A collisions (closed symbols) and inelastic p+p(\bar{p}) interactions (open symbols). The results of NA49 are indicated by squares. The insert shows the difference between the results for A+A collisions and the straight line parametrisation of p+p(\bar{p}) data (dashed line). The solid line shows a straight line fit to the results on high energy (158 A·GeV and above) central Pb+Pb and Au+Au collisions. The inner error bars on the NA49 points are statistical and the outer systematic.

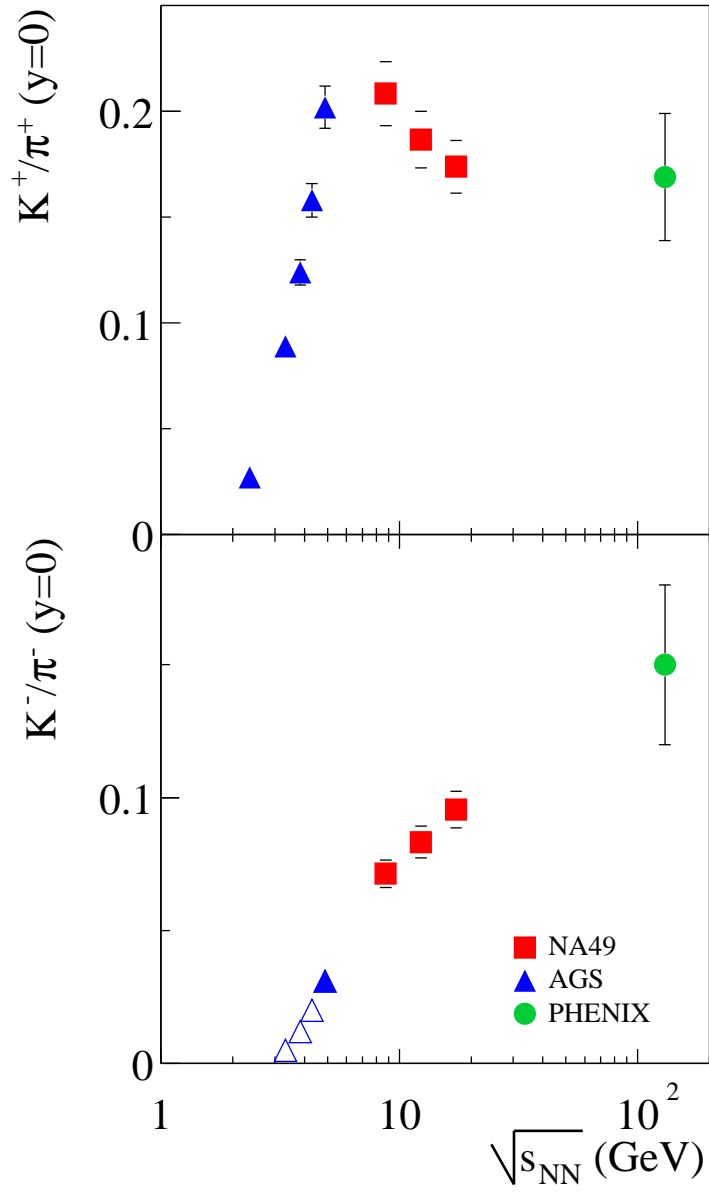


FIG. 5. The energy dependence of the midrapidity K^+/π^+ and K^-/π^- ratios in central Pb+Pb and Au+Au collisions. The results of NA49 are indicated by squares. Open triangles indicate the A+A results for which a substantial extrapolation was done. The error bars on the NA49 points are systematic, the statistical errors are smaller than the symbol size.

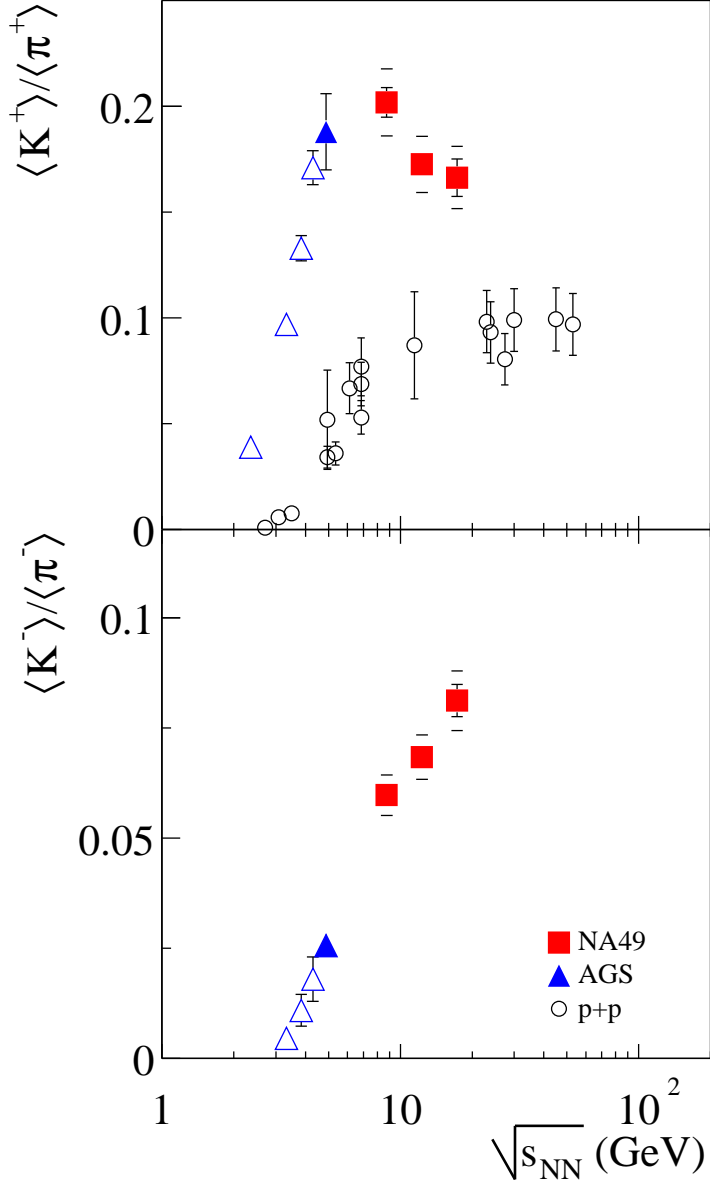


FIG. 6. The energy dependence of full phase space $\langle K^+ \rangle / \langle \pi^+ \rangle$ and $\langle K^- \rangle / \langle \pi^- \rangle$ ratios in central Pb+Pb (Au+Au) collisions. The results of NA49 are indicated by squares. The data for p+p interactions are shown by open circles for comparison. Open triangles indicate the A+A results for which a substantial extrapolation was necessary. The inner error bars on the NA49 points are statistical and the outer systematic.

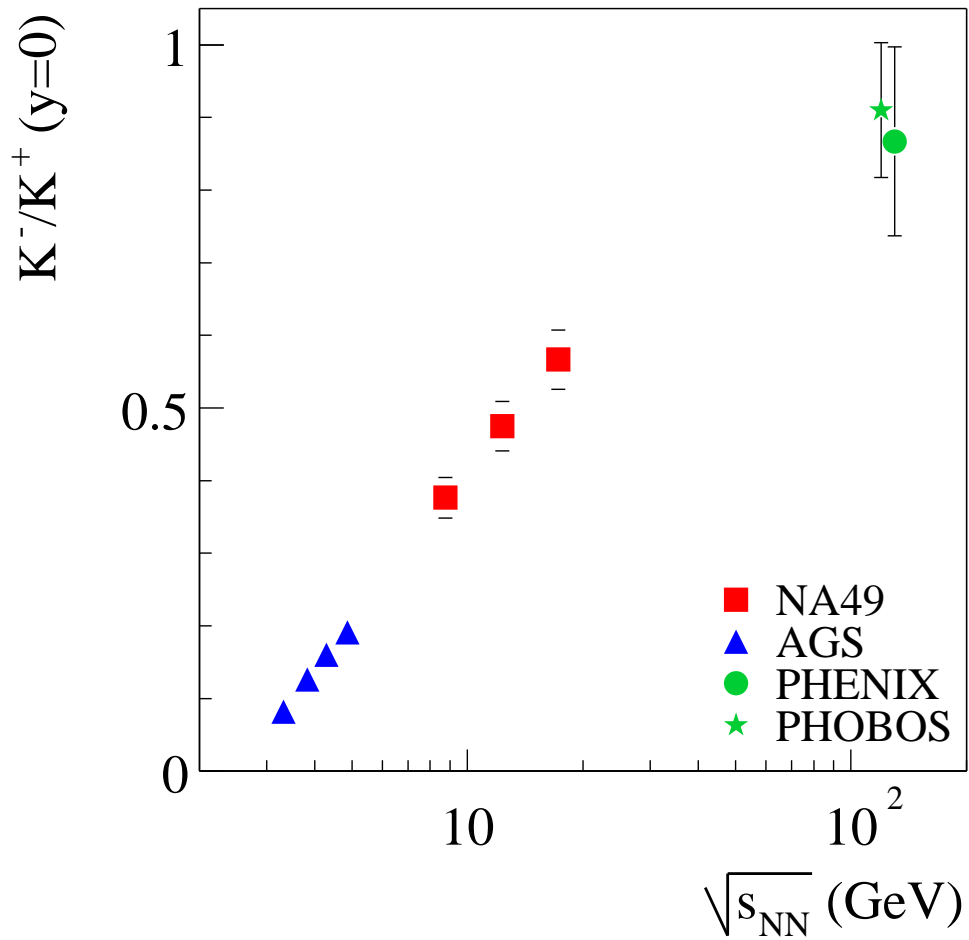


FIG. 7. The energy dependence of the midrapidity K^-/K^+ ratio in central Pb+Pb (Au+Au) collisions. The results of NA49 are indicated by squares. The error bars on the NA49 points are systematic, the statistical errors are smaller than the symbol size.

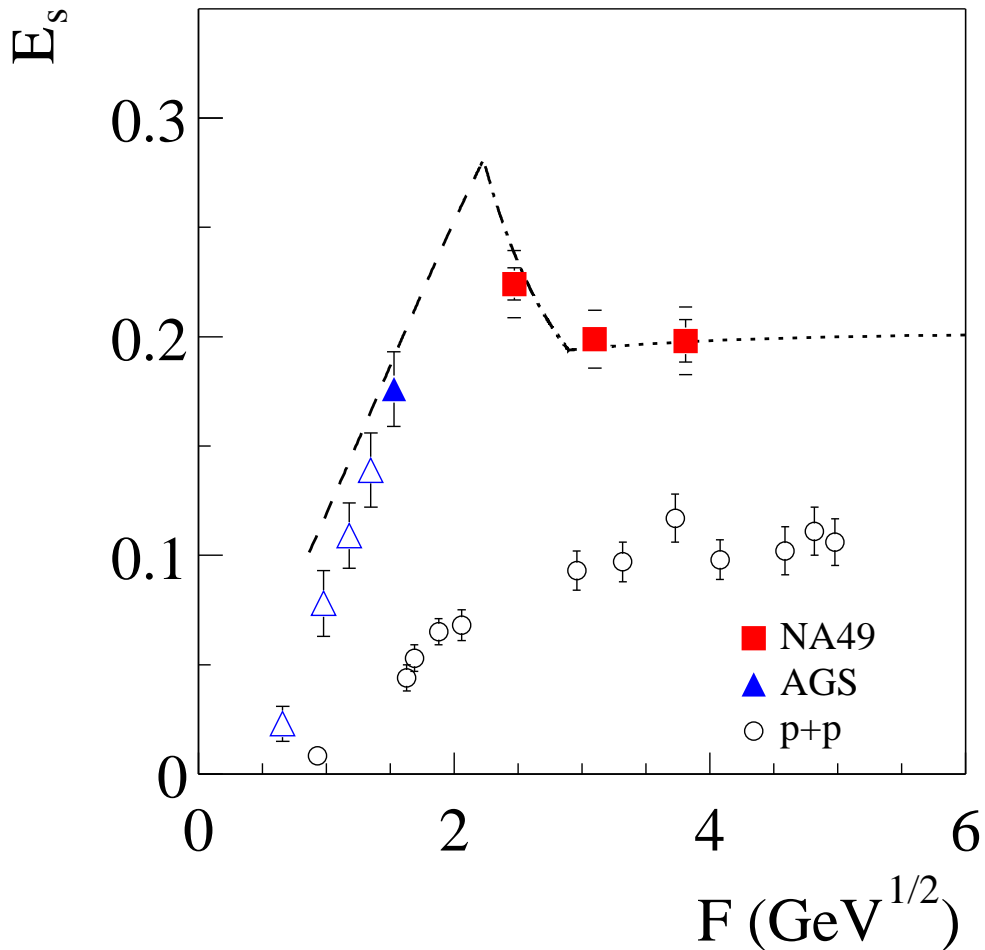


FIG. 8. The energy dependence of the $E_S = (\langle\Lambda\rangle + \langle K + \bar{K}\rangle)/\langle\pi\rangle$ ratio in central Pb+Pb (Au+Au) collisions and p+p interactions. Open triangles indicate the A+A results for which a substantial extrapolation was necessary. The experimental results on A+A collisions are compared with the predictions of the Statistical Model of the Early Stage (line) [5]. Different line styles indicate predictions for energy domains in which confined matter (dashed line), mixed phase (dash-dotted line) and QGP (dotted line) are created at the early stage of the collisions. The non-monotonic behaviour of the E_S ratio in the model is due to the crossing of the threshold energy for QGP creation in the early stage of A+A collisions. The inner error bars on the NA49 points are statistical and the outer systematic.

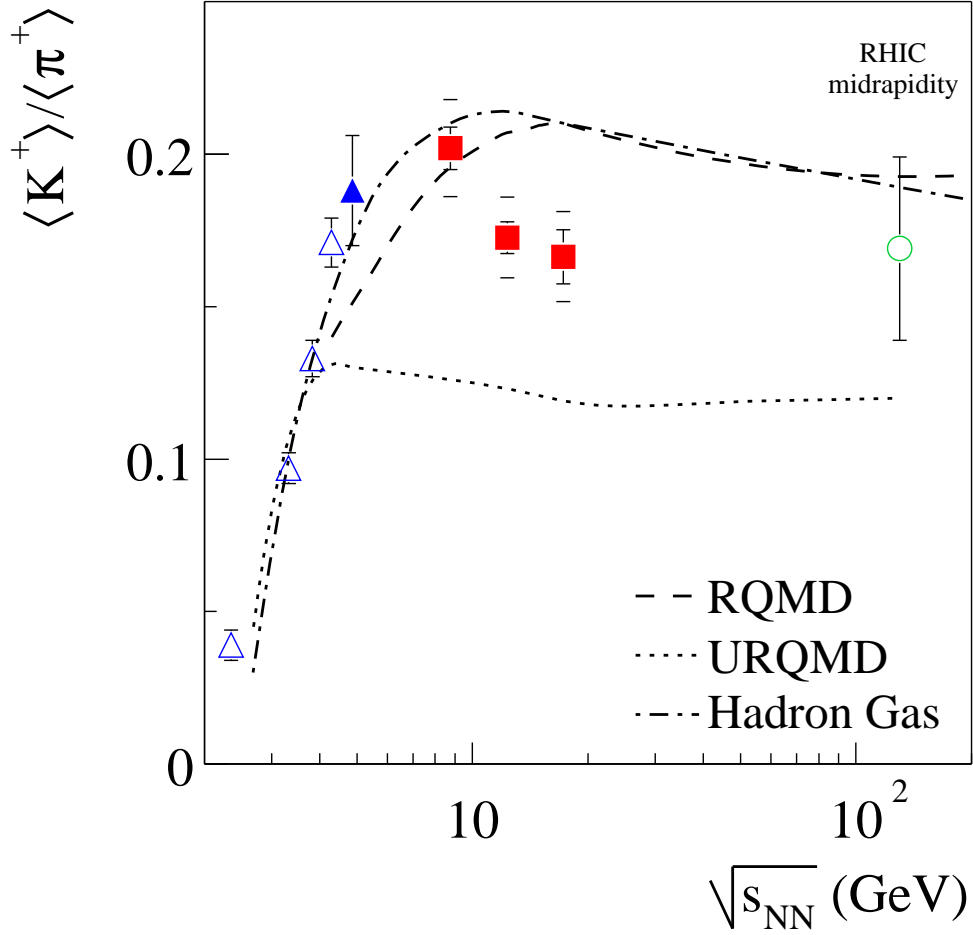


FIG. 9. The energy dependence of the full phase space $\langle K^+ \rangle / \langle \pi^+ \rangle$ ratio in central Pb+Pb and Au+Au collisions. The experimental results taken from Fig. 6 are compared to model predictions: RQMD [31] (dashed line), UrQMD [33] (dotted line) and the Extended Hadron Gas Model [29] (dash-dotted line).

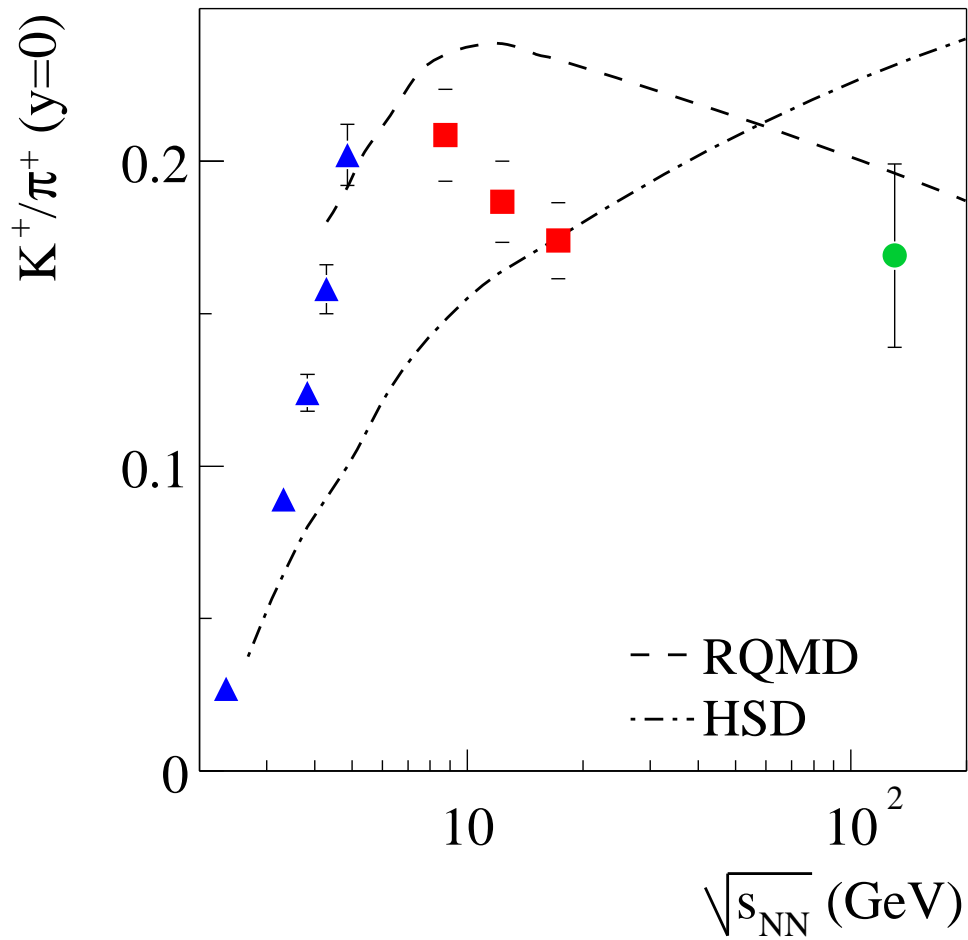


FIG. 10. The energy dependence of the midrapidity K^+/π^+ ratio in central Pb+Pb and Au+Au collisions. The experimental results taken from Fig. 5 are compared with model predictions: RQMD [31] (dashed line) and HSD [35] (dash-dotted line).